J Mol Model (2010) 16:1895–1909
DOI 10.1007/s00894-010-0682-z

ORIGINAL PAPER

Theoretical study of Z isomers of A-type dimeric proanthocyanidins substituted with R=H, OH and OCH_3: stability and reactivity properties

Erika N. Bentz · Alicia H. Jubert · Alicia B. Pomilio · Rosana M. Lobayan

Received: 30 October 2009 / Accepted: 21 January 2010 / Published online: 17 March 2010

Abstract The stereochemistry of A-type dimeric proanthocyanidins was studied, focusing on the factors that determine it, and the changes that occur with R = OCH_3, R′ = H, and R = OH, R′ = H as substituents, starting with the study of the conformational space of each species. Using molecular dynamics at a semiempirical level, and complementing with functional density calculations, two conformers of lowest energy were characterized for R = H, eight conformers for R = OH, and three conformers for R = OCH_3. Electronic distributions were analyzed at a higher calculation level, thus improving the basis set. Intramolecular interactions were examined and characterized by the theory of atoms in molecules (AIM). Detailed natural bond orbitals (NBO) analysis allowed the description of subtle stereoelectronic aspects of fundamental importance for understanding the stabilization and antioxidant function of these structures. The study was enriched by a deep analysis of maps of molecular electrostatic potential (MEP). The coordinated analysis of MEP, together with the NBO and AIM results, allowed us to rationalize novel distribution aspects of the potential created in the space around a molecule.

Keywords Dimeric proanthocyanidins · Density functional theory · Atoms in molecules · NBO analysis · Topological properties · Maps of electrostatic potential

Electronic supplementary material The online version of this article (doi:10.1007/s00894-010-0682-z) contains supplementary material, which is available to authorized users.

E. N. Bentz · R. M. Lobayan (✉)
Facultad de Ingeniería, Universidad de la Cuenca del Plata,
Lavalle 50,
3400 Corrientes, Argentina
e-mail: rlobayan@ucp.edu.ar

A. H. Jubert
CEQUINOR Facultad de Ciencias Exactas y Facultad de Ingeniería, Universidad Nacional de La Plata,
CC 962,
1900 La Plata, Argentina

A. B. Pomilio
PRALIB (UBA, CONICET), Facultad de Farmacia y Bioquímica,
Universidad de Buenos Aires,
Junín 956,
C1113AAD Buenos Aires, Argentina

Introduction

Procyanidins are organic compounds found in some vascular plants, and have been synthesized as simple and dimeric molecules with a variety of substituents in the aromatic rings [1]. Their antioxidant activity is well documented, but there are no crystallographic data [2–6].

The interest in these compounds arises from the fact that one of their most important applications is in the stabilization of suspensions, which is useful in the food industry, mainly in the processing of citrus juices [1, 7]. Depending on the position of the ether bridge, dimeric procyanidins may have A- or B-type structures.

We previously reported [8] a conformational and electronic study of the A-type dimeric proanthocyanidin with R, R′ = H (Fig. 1), which has an intramolecular plane of symmetry. The occurrence of both C and E rings, and the C-3–H2 bridge, markedly decreases the flexibility of the molecule. The main substructure of this molecule is a bicyclic structure consisting of two six-membered rings (C and E), where each involves a benzo-γ-pyran group, fused by the C-3–H2 bridge, with both C-2 and C-4 as

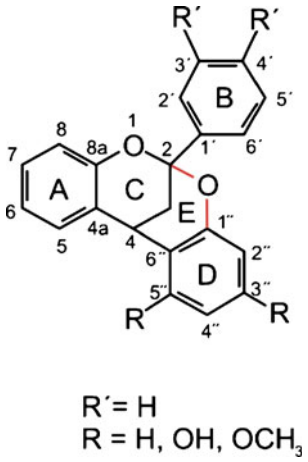

Fig. 1 Structure of Z- isomers of A-type dimeric proanthocyanidin substituted with R = H, OH, OCH_3. Atom numbering is indicated

bridgeheads. Consequently, this bridge is a stereo-center resulting in an E/Z isomerism, depending on the configuration of Ph-2 and H-4, and any other substituent at those positions.

Scanning of the conformational space for R, R′ = H revealed two lowest energy conformers for the Z-isomer, and only one conformer for the E-isomer. The steric hindrance and high tension of the C and D rings characterize the E-isomer, thus giving rise to a higher energy for this isomer than that for Z [8].

Given its higher stability, the present study examines the effects of substitution on the Z-isomer, including R = OCH_3, R′ = H, and R = OH, R′ = H (Fig. 1).

The conformational space of the substituted stereoisomers of A-type procyanidin was scanned using molecular dynamics (MD) calculations, and further density calculations at the B3LYP level and 6-31G** basis were performed to optimize the geometry of the lowest-energy conformers of each species obtained in these simulations.

Maps of molecular electrostatic potential (MEP) were also obtained. The electronic distribution of the conformers was analyzed at the B3LYP/6-311++G** level, with intramolecular interactions being studied and characterized by the theory of atoms in molecules (AIM). The study was complemented by natural bond orbital (NBO) analysis.

The scant knowledge of the structural features of these compounds called for this analysis to be applied to their stereochemistry, advancing description of the factors that determine it, and the changes that occur upon substitutions with R = OCH_3, R′ = H, and R = OH, R′ = H. This analysis was designed to describe the stabilization and possible interactions with other organic molecules in a food matrix. Owing to the complexity of these molecules (presence of two prochiral carbons, and a rigid [3.1.3]-bicyclic substructure) a step-by-step analysis through an order of increasing complexity has been proposed, this work being the second in a series of studies (see [8] for first in series) with the ultimate aim of studying polymeric species.

Methods

The study of conformational space was performed by MD calculations using a module of the HyperChem software package [9]. Several simulations were carried out with the aid of the MM + force field. The input geometries were heated from 0 to 800 K in steps of 0.1 ps. Then, the temperature was kept constant by coupling the system to a simulated thermal bath with a relaxation time of 0.5 ps. The simulation time step was 0.5 fs. After an equilibration period of 1 ps, a simulation of 500 ps was performed, retaining atomic coordinates every 1 ps. These geometries were then optimized to an energy gradient less than 0.01 kcal mol^{-1} A^{-1} by the AM1 method.

The lowest energy conformers were studied using density functional theory (DFT) as implemented in the Gaussian 03 software package [10]. Total geometry optimization was performed with the three-parameter hybrid functional of Becke with the correlation functional of Lee-Yang-Parr. This combination gave rise to the well-known B3LYP method. The 6-31G** basis set was used for all atoms.

MEP maps were obtained in the van der Waals molecule surfaces using the Gaussian 03 software, and were further visualized using MOLEKEL 4.0 [11].

The topological analysis was performed with modules of the AIMPAC package [12], using wave functions obtained at the B3LYP level and 6-311++G** basis set. NBO analysis was performed at the same level [13].

Results and discussion

The study of the conformational space led to two conformers of lowest energy for R = H [8] (Fig. 2), eight

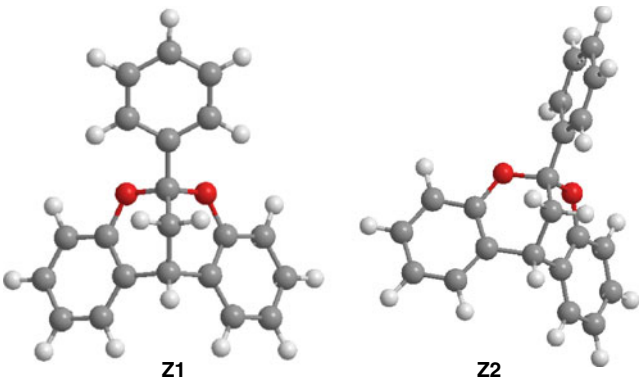

Fig. 2 Optimized geometry of both conformers of the Z-isomer of A-type dimeric proanthocyanidin at B3LYP/6-31G** level. Geometries were confirmed as local minima by vibrational analysis

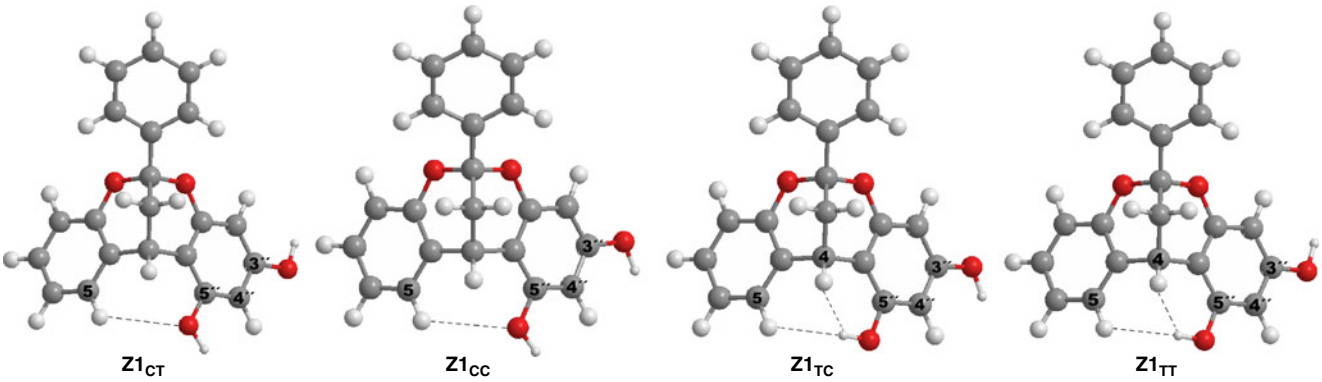

Fig. 3 Optimized geometry of conformers of the Z-isomer of A-type dimeric proanthocyanidin substituted with R′ = H, R = OH at B3LYP/6-31G** level of theory. *Dashed lines*: Intramolecular hydrogen bond interactions. Only Z1 conformers are shown

conformers for R = OH (Fig. 3), and three conformers for R = OCH_3 (Fig. 4). These structures have been confirmed as minima by the absence of negative frequencies.

The energy values and internal coordinates of the conformers under study are shown in Table 1. The conformers of the R = H species show a high symmetry, the geometric parameters of ring A being similar to those of ring D. As expected, this symmetry is lost when substituted with R = OH, and R = OCH_3 (Table 1).

The C-3—C-2—C-1′—C-6′ dihedral angle in relation to the position of ring B has a mean value of 88° for a set of structures called the Z1 group, and close to 0° for the other, Z2, group. Therefore, the conformers are defined as Z1 and Z2 conformers, respectively (Fig. 2).

Analysis of the H—O-3″—C-3″—C-4″ and H—O-5″—C-5″—C-4″ dihedral angles is suitable for distinguishing conformers whose mean values are either close to 180° (anti position) or close to 0° (syn position). The "T" and "C" subscripts for the conformers refer to trans (anti) or cis (syn) configuration in relation to the C-3″—C-4″ and C-5″—C-4″ bonds, respectively (Figs. 3, 4).

Regardless of the substitution, the energy values show that Z1 conformers are on average 1.88 kcal mol^{-1} more stable than Z2. For all conformers, the angles between the bonds that define rings C and E, and their respective lengths, are very similar for both Z1 and Z2 conformers. However, there is a remarkable difference in the C-3—C-2—C-1′ angle, which averages 112.7° for Z1, and 116.6° for Z2. Although this angle differs by about 4°, Z2 can be considered a rotamer of Z1 with respect to an axis through the C-1′—C-2 bond in all species under study.

For R = OH, the energy value found for the most stable conformer, called $Z1_{CT}$ (Fig. 3), was −697,033.86 kcal mol^{-1}. The energy differences for the other conformers with respect to the most stable were 0.63 kcal mol^{-1} for $Z1_{CC}$, and 2.51 kcal mol^{-1} for $Z1_{TC}$ and $Z1_{TT}$. The energy differences for Z2 conformers were 1.88 kcal mol^{-1} for $Z2_{CT}$, 2.51 kcal mol^{-1} for $Z2_{CC}$, and 4.39 kcal mol^{-1} for both $Z2_{TC}$ and $Z2_{TT}$.

The energy value found for the most stable conformer with R=OCH_3 ($Z1_{CT}$; Fig. 4) was −746,362.16 kcal mol^{-1}, and the energy differences for the other conformers were 1.25 kcal mol^{-1} for $Z1_{CC}$, and 3.07 kcal mol^{-1} for $Z2_{CC}$.

The "CT" conformers were 0.63 kcal mol^{-1} (1.25 kcal mol^{-1}) more stable than "CC" for R=OH (R=OCH_3). These trends are rationalized below in the section on NBO analysis.

"TC" and "TT" conformers were not described for R = OCH_3 (steric hindrance), but these conformers did exist for R = OH, and showed the same energy.

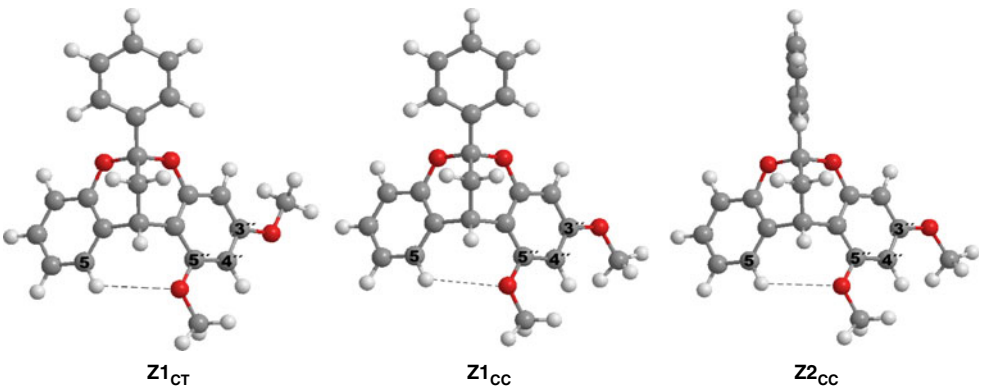

Fig. 4 Optimized geometry of conformers of the Z-isomer of A-type dimeric proanthocyanidin substituted with R′ = H, R = OCH_3 at B3LYP/6-31G** level of theory. *Dashed lines*: Intramolecular hydrogen bond interactions

Topology of the electronic charge density

The AIM theory [14] is based on the analysis of critical points (CP) of molecular charge density, ρ [15, 16]. At these points, the gradient of the electronic density, $\nabla^2 \rho$, is null and is characterized by the three eigenvalues, λ_i (i=1–3) of the ρ Hessian matrix. The CPs were named and classified as (r, s) according to their rank, r (number of nonzero eigenvalues), and signature, s (the algebraic sum of the three eigenvalues). Several properties evaluated at the bond CP [BCP, a (3,−1) CP] constitute powerful tools to classify a given chemical structure. The negative eigenvalues of the Hessian matrix (λ_1 and λ_2, respectively) measure the degree of contraction of ρ at a normal direction to the bond towards the CP, while a positive eigenvalue (i.e., λ_3) gives a quantitative indication of the contraction degree parallel to the bond and from the CP towards each of the neighboring nuclei. When the positive eigenvalues are dominant, the electronic density is concentrated locally at each atomic basin. The interaction is classified as closed shell and is typical of highly ionic bonds, hydrogen bonds, and van der Waals interactions. This particular interaction is described by relatively low $\nabla^2\rho_b$ values, $\nabla^2\rho_b>0$ and $|\lambda_1|/\lambda_3<1$ and $G_b>1$. Another interesting parameter is the ellipticity, ε, defined as λ_1/λ_2-1. Ellipticity is indicative of the similarity between perpendicular curvatures (λ_1 and λ_2) at BCP, and measures the extent to which density is preferentially accumulated in a given plane containing the bond path. If $\lambda_1=\lambda_2$, then $\varepsilon=0$, and the bond is cylindrically symmetric, e.g., a C–C single bond in ethane, and a triple bond in acetylene.

As supplementary material, the values of electron charge density (ρ_b), Laplacian of charge density ($\nabla^2 \rho_b$), Hessian matrix eigenvalues (λ_1, λ_2 and λ_3), ellipticity (ε), kinetic energy density (G_b), and the $|\lambda_1|/\lambda_3$ and G_b/ρ_b relationships, in BCPs for all expected chemical bonds of the lowest energy conformers obtained by substituting R = OH and R = OCH_3 are shown (Tables S1 and S2, respectively).

According to the AIM theory, when negative eigenvalues dominate, the electronic charge is locally concentrated in the CP region, which leads to polar covalent interactions. These are characterized by high ρ_b values, $|\lambda_1|/\lambda_3>1$ and $G_b/\rho_b<1$, and large, less than zero, Laplacian values, indicating charge accumulation between the bound nuclei [14].

For all studied conformers this behavior occurs in C–H bonds, and all C–C bonds of rings A, B, and D. The C-2—O1 bond of ring C also shows the same behavior typical of a covalent bond, which is due, as previously demonstrated [8], to the change of C-2 hybridization (from sp^2 to sp^3), when the γ-pyran is formed.

The C-8a—O1 bond of ring C, and the equivalent for ring E, C-1″—O1 and C—O bonds accounting for R = OCH_3 and R = OH, do not behave like C-2—O1, since they show values corresponding to an intermediate or shared polar covalent bond (high ρb, large and less than zero $\nabla^2\rho_b$, $|\lambda_1|/\lambda_3<1$, and $G_b/\rho_b>1$).

We found that this behavior is typical of C—O bonds in the pyranose ring, where the C atom also has sp^2 hybridization. The C-8a—O1 BCP topological features are a consequence of the charge density redistribution due to the conjugation of O1 lone pairs with the π-orbitals [8].

Hydrogen-bond intramolecular interactions have been also characterized in the substituted species. The occurrence of a hydrogen bond is associated with the BCP formation between the H atom and the acceptor atom (A) involved [17, 18]. This CP has properties that are typical of a closed shell interaction. In particular, the following hydrogen bond interactions have been characterized: (1) H···O type (in $Z1_{CT}$, $Z1_{CC}$, $Z2_{CT}$ and $Z2_{CC}$ conformers for R = OH, and in all conformers for R = OCH_3), and (2) dihydrogen-type: C-5—H-5···H-5″—O5″ and C-4—H-4···H-5″—O5″ (in $Z1_{TC}$ and $Z1_{TT}$, R = OH), and C-5—H-5···H-5″ (in $Z2_{TC}$ and $Z2_{TT}$, R = OH). These interactions are shown with dotted lines in Figs. 3 and 4. Some relevant geometric parameters of these interactions, such as the distances H···O, H···H, C···O, and the C—H···Y, Y = O, H bond angle are shown in Table 2. The formation of the H-bonds H-5···O-5″, H-5″···H-5 and H-5″···H-4 closes seven-membered, eight-membered, and six-membered rings, respectively, and is accompanied by the appearance of ring critical points (RCPs), as required for the satisfaction of the Poincaré-Hopf relationship [14]. Local topological properties calculated in the respective BCP and RCP are listed in Table 3.

The H···O type hydrogen bonds with distances around 2.80–2.93 Å (in the expected range of 2–3 Å for C—H···O bonds) were found in all conformers of the substituted structures, except for "TC" and "TT" with R = OH. According to other authors [19], the shorter the interatomic H···A distance, and closer to 180° the D—H···A angle, the higher the strength of the hydrogen bond interaction. Another parameter that characterizes this type of bond as a weak hydrogen bond is the distance between the C atom attached to the hydrogen of the bridge, and the O oxygen atom (in the range of 3.41–3.54 Å) [19]. The bond angle between donor and acceptor atoms (C—H···O) varies in the range 114.7–115.3°—also in agreement with this classification. The electron density values are lower than those expected for typical intramolecular hydrogen bonds (expected densities about 0.02–0.03 a.u.) [17, 20] (see Table 3). Taking into account the correlation between the BCP density and the interaction strength [18], from the analysis of topological parameters it can also be concluded that this interaction is typically weak, contributing very little to structure stabilization. $\nabla^2\rho_b$ varies in the range of 0.015–0.016 a.u. (0.016–0.017 a.u. for R = OCH_3),

Table 1 Relevant internal coordinates and ΔE of conformers of the Z-isomer of A-type dimeric proanthocyanidin substituted with R′=H, R=OH and R=OCH_3 calculated at the B3LYP/6-31G** level of theory

	R=OH								R=OCH_3		
	$Z1_{CT}$	$Z1_{CC}$	$Z1_{TC}$	$Z1_{TT}$	$Z2_{CT}$	$Z2_{CC}$	$Z2_{TC}$	$Z2_{TT}$	$Z1_{CT}$	$Z1_{CC}$	$Z2_{CC}$
ΔE (kcal mol^{-1})	0	0.63	2.51	2.51	1.88	2.51	4.39	4.39	0	1.3	3.1
Dihedral angles (°)											
C-3—C-2—C-1′—C-6′	88.2	89.6	90.3	88.9	3.6	1.6	–3.4	–2.0	88.3	88.9	0.2
C-3—C-2—C-1′—C-2′	–88.2	–86.9	–86.2	–87.6	–176.7	–178.5	176.9	178.0	–88.1	–87.3	–179.8
O1—C-2—C-1′—C-2′	33.8	35.0	35.6	34.3	–53.3	–55.3	–58.9	–57.6	33.9	34.6	–56.7
H—O-5′′—C-5′′—C-4′′	0.1	0.2	–176.6	–176.8	0.1	0.1	–153.6	–152.6	—	—	—
H—O-3′′—C-3′′—C-4′′	179.2	0.8	0.4	179.1	179.6	0.7	–0.8	178.7	—	—	—
C-3a′′—O-3′′—C-3′′—C-4′′	—	—	—	—	—	—	—	—	0.8	1.1	0.7
C-5a′′—O-5′′—C-5′′—C-4′′	—	—	—	—	—	—	—	—	179.2	0.7	0.6
Angles (°)											
C-3—C-2—C-1′	112.8	112.8	112.6	112.7	116.6	116.5	116.6	116.6	112.7	112.7	116.6
C-2—C-3—C-4	107.5	107.5	107.4	107.4	107.5	107.4	107.2	107.2	107.5	107.5	107.4
C-8a—O1—C-2	120.4	120.4	120.6	120.6	120.8	120.7	121.5	121.5	120.4	120.4	120.7
C-4a—C-8a—C-8	121.0	29.4	120.9	29.5	121.0	121.0	127.6	120.8	121.0	121.0	121.0
O1—C-2—O	109.0	109.1	109.1	109.1	108.4	108.4	108.0	108.0	109.1	109.1	108.5
C-4a—C-8a—O1	122.8	116.0	122.9	122.9	122.6	122.6	122.2	122.2	122.8	122.8	122.7
C-4a—C-4—C-8a	117.9	93.7	117.6	117.6	117.7	117.7	116.4	116.4	117.9	117.9	117.8
C-4a—C-4—C-3	107.7	131.4	107.6	107.6	107.8	107.8	106.7	106.7	107.6	107.6	107.9
C-3—C-4—H	110.9	110.9	109.0	109.0	110.5	110.5	109.8	109.8	110.9	110.9	110.5

comparable with previous results (0.016 to 0.139 a.u.). Ellipticity varies around 0.256–0.273 (0.239–0.261 for R = OCH_3), the smallest values being for Z2.

The non-conventional dihydrogen-type bonds as well as the conventional hydrogen bonds such as those described above, may occur either as intermolecular or intramolecular bonds.

A dihydrogen bond always comprises an electronegative atom (X) on one side, and an electropositive atom (Y) on the other side, $X—H^{+\delta}\cdots{}^{-\delta}H—Y$. Spectroscopic studies indicate that the H···H distance in such systems is typically 1.7–2.2 Å [21]. Dihydrogen bonds appear in "TC" and "TT" conformers for R=OH, for both Z1 and Z2, and occur among H-5, H-4 and H-5″. Multiple dihydrogen bonds [22] were characterized in $Z1_{TC}$ and $Z1_{TT}$. For these two conformers, the H-5—H-5" distance is 2.33 Å, and that of H-4—H-5" is 1.97 Å. The angle between the donor atom and the hydric hydrogen $^{-\delta}H$ ($O—H^{+\delta}\cdots{}^{-\delta}H$) is higher

Table 2 Relevant internal coordinates for hydrogen bonds in conformers substituted with R′ = H, R = OH and R = OCH_3 calculated at the B3LYP/6-31G** level of theory[a]

		R′=H R=OH								R′=H R=OCH_3		
		$Z1_{CT}$	$Z1_{CC}$	$Z1_{TC}$	$Z1_{TT}$	$Z2_{CT}$	$Z2_{CC}$	$Z2_{TC}$	$Z2_{TT}$	$Z1_{CT}$	$Z1_{CC}$	$Z2_{CC}$
H-5···O-5″	H-5···O-5″	2.94	2.94	3.14	3.13	2.80	2.93	3.16	3.16	2.92	2.92	2.91
	C-5···O-5″	3.54	3.54	3.70	3.69	3.41	3.53	3.58	3.59	3.51	3.51	3.51
	C-5—H-5···O-5″	115.09	115.25	—	—	114.68	114.77	—	—	114.89	114.92	114.92
H-5···H-5″	H-5···H-5″	3.61	3.61	2.34	2.34	3.60	3.60	2.19	2.19	—	—	—
	C-5—H5···H-5″	123.11	123.33	117.08	116.91	122.67	122.79	104.03	103.84	—	—	—
	H-5···H-5′′—O-5″	—	—	139.58	139.32	—	—	175.46	174.05	—	—	—
H-4···H-5″	H-4···H-5″	3.43	3.43	1.97	1.97	3.43	3.43	2.23	2.24	—	—	—
	C-4—H-4....H-5″	101.73	101.85	104.10	104.02	101.52	101.59	93.24	93.03	—	—	—
	H-4···H-5′′—O-5″	—	—	128.89	129.54	—	—	106.95	106.05	—	—	—

[a] Bond lengths are expressed in Å, angles and dihedral angles in degrees

Table 3 Topological properties at bond critical point (BCP) for hydrogen bonds in conformers substituted with R′ = H, R = OH and R = OCH_3 calculated at the B3LYP/6-311++G** level of theory. Relevant topological properties at (3, +1) BCP for the corresponding rings are also reported[a]

BCP				Bond length	ρ_b	$\nabla^2\rho_b$	λ_1	λ_2	λ_3	ε	G_b/ρ_b	V_b	H_b
(3, -1)	OH	$Z1_{CT}$	H5···O5″	2.938	0.004	0.016	–0.003	–0.002	0.021	0.273	0.770	–0.002	0.001
		$Z1_{CC}$	H5···O5″	2.939	0.004	0.016	–0.003	–0.002	0.021	0.275	0.774	–0.002	0.001
		$Z1_{TC}$	H5···H5″	2.337	0.005	0.018	–0.004	–0.002	0.023	0.944	0.702	–0.003	0.001
		$Z1_{TC}$	H4···H5″	1.972	0.014	0.050	–0.014	–0.006	0.070	1.287	0.785	–0.009	0.002
		$Z1_{TT}$	H5···H5″	2.337	0.005	0.018	–0.004	–0.002	0.023	0.956	0.703	–0.003	0.001
		$Z1_{TT}$	H4···H5″	1.968	0.014	0.051	–0.014	–0.006	0.071	1.242	0.784	–0.009	0.002
		$Z2_{CT}$	H5···O5″	2.802	0.004	0.016	–0.003	–0.002	0.021	0.256	0.769	–0.003	0.001
		$Z2_{CC}$	H5···O5″	2.933	0.004	0.016	–0.003	–0.002	0.021	0.255	0.771	–0.003	0.001
		$Z2_{TC}$	H5···H5″	2.192	0.007	0.024	–0.006	–0.004	0.034	0.518	0.652	–0.003	0.001
		$Z2_{TT}$	H5···H5″	2.193	0.007	0.024	–0.006	–0.004	0.034	0.530	0.652	–0.003	0.001
	OCH_3	$Z1_{CT}$	H5···O5″	2.919	0.004	0.017	–0.003	–0.002	0.022	0.261	0.764	–0.003	0.001
		$Z1_{CC}$	H5···O5″	2.918	0.004	0.017	–0.003	–0.002	0.022	0.264	0.766	–0.003	0.001
		$Z2_{CC}$	H5···O5″	2.913	0.005	0.017	–0.003	–0.002	0.022	0.240	0.765	–0.003	0.001
(3,+1)	OH	$Z1_{CT}$			0.004	0.017	–0.002	0.003	0.015	—			
		$Z1_{CC}$			0.004	0.017	–0.002	0.003	0.015	—			
		$Z1_{TC}$			0.005	0.018	–0.003	0.002	0.019	—			
		$Z1_{TC}$			0.014	0.060	–0.012	0.007	0.064	—			
		$Z1_{TT}$			0.005	0.018	–0.003	0.002	0.019	—			
		$Z1_{TT}$			0.014	0.060	–0.012	0.008	0.065	—			
		$Z2_{CT}$			0.004	0.017	–0.001	0.003	0.015	—			
		$Z2_{CC}$			0.004	0.017	–0.001	0.003	0.015	—			
		$Z2_{TC}$			0.007	0.025	–0.003	0.005	0.023	—			
		$Z2_{TT}$			0.007	0.025	–0.003	0.005	0.023	—			
	OCH_3	$Z1_{CT}$			0.004	0.018	–0.002	0.004	0.016	—			
		$Z1_{CC}$			0.004	0.018	–0.002	0.004	0.016	—			
		$Z2_{CC}$			0.004	0.018	–0.002	0.004	0.016	—			

[a] ρ_b,$\nabla^2\rho_b$, G_b/ρ_b, λ_1, λ_2, λ_3 are expressed in a.u. and bond lengths in Å

(more linear, it varies around 150–170°) than the angle associated with the protic hydrogen $H^{+\delta}\cdots{}^{-\delta}H$—C (more bent, it varies around 95–115°) as expected for such interactions [23]. The BCP topological parameter values and the difference found in the value of natural charges for the hydrogen atoms involved ($\Delta q \approx 0.3$ a.u.) led to closed shell weak electrostatic interactions [24, 25].

By subtracting structures the stabilizing effect (1.88 kcal mol^{-1}) associated with the position of ring B (Δ=4.39 kcal mol^{-1}−1.88 kcal mol^{-1}=2.51 kcal mol^{-1}) in Z2, it was shown that the stabilizing effect of dihydrogen interactions is similar in all cases.

NBO analysis

NBO analysis transforms the canonical delocalized Hartree-Fock (HF) molecular orbitals (MOs), or corresponding natural orbitals of a correlated description, into localized orbitals that are closely linked to chemical bonding concepts.

Filled NBOs describe the hypothetical, strictly localized Lewis structure. The interactions between filled and vacant orbitals account for the deviation of the molecule from the Lewis structure and can be used as a measure of delocalization. This method provides energies of hyper-conjugative interactions from the second-order perturbation approach

$$E^{(2)} = -n_i \frac{F_{ij}^2}{\varepsilon_j - \varepsilon_i} \quad (1)$$

where F_{ij} is the Fock matrix element between the i and j NBO orbitals, ε_i and ε_j are the energies of i and j NBOs, and n_i is the population of the donor i orbital.

The structures under study showed nearly the same second-order stabilization energies for $1n_{O1}\rightarrow\sigma^*_{C\text{-}8a—C\text{-}8}$ transfers (0.55 kcal mol^{-1} on average). Energies associated with $1n_{O1}\rightarrow\ \sigma^*_{C\text{-}8a—C\text{-}4a}$ and $2n_{O1}\rightarrow\pi^*_{C\text{-}8a—C\text{-}4a}$ transfers are 7.12 kcal mol^{-1} and 26.12 kcal mol^{-1}, respectively, on average. The R=H conformers have symmetric contributions

to these energies accounting for the resonance of the O oxygen with ring D. However, in the case of substituted species, this symmetry is broken, and hyperconjugative interactions related to O are now $1n_{O\rightarrow}\ \sigma^*_{C\text{-}1''\text{—}C\text{-}2''}$ (0.56 kcal mol^{-1} on average), $1n_{O\rightarrow}\ \sigma^*_{C\text{-}1''\text{—}C\text{-}6''}$ (6.87 kcal mol^{-1} on average), and $2n_{O\rightarrow}\pi^*_{C\text{-}1''\text{—}C\text{-}2'}$ (26.88 kcal mol^{-1} on average). This information describes the resonance of oxygen lone pairs with rings A and D.

Bond polarization or ionicity is described by NBO calculations of the electron density percentage on each atom of the bond (Table 4). The results indicate that in substituted compounds (for R=H there is almost no change) the C-2—C-3 polarization is higher than that of the C-3—C-4 bond. On the other hand, upon comparison of $Z1_{CT}$ for R=OH and $Z1_{CT}$ for R = OCH_3, it is evident that the C-2—C-3 polarization increases according to R = H < R = OCH_3 < R = OH.

It is remarkable that this behavior associated with conformational effects was correlated with relative structure stability (Z1 conformers are more stable than Z2, "CT" are more stable than "CC", which are in turn more stable than both "TC" and "TT"). In other words, at higher C-2—C-3 polarization, higher structural stability is expected.

For R = OCH_3, the second-order stabilization energy of the $\sigma_{C\text{-}3''a\text{—}O\text{-}3''} \rightarrow \sigma^*_{C\text{-}3''\text{—}C\text{-}4''}$ transfer is higher in the "CT" conformer than in "CC" (3.11 kcal mol^{-1} and 2.93 kcal mol^{-1}, respectively; Table 5). This indicates a higher electron delocalization in "CT", and explains its relative stabilization ($\Delta E_{Z1CT\text{-}Z1CC}$: 1.25 kcal mol^{-1}; Table 1). Similarly, for R = OH, the $\sigma_{H\text{—}O\text{-}3''\rightarrow}\ \sigma^*_{C\text{-}3''\text{—}C\text{-}4''}$ transfer (5.15 kcal mol^{-1} and 4.98 kcal mol^{-1}; Table 6; $\Delta E_{Z1CT\text{-}Z1CC}$: 0.63 kcal mol^{-1}; Table 1); H is designated the hydrogen atom of the substituent.

The highest stabilization for R = OCH_3 is explained by the major efficiency of the $\sigma_{C\text{-}3''C\text{-}4''} \rightarrow \sigma^*_{C\text{-}5''\text{—}O\text{-}5''}$ transfer, to which second-order stabilization energies of 5.06 kcal mol^{-1} in "CT", and 4.68 kcal mol^{-1} in "CC" are associated, while for R = OH the respective energies are 4.67 kcal mol^{-1} in "CT" and 4.56 kcal mol^{-1} in "CC" (Tables 5, 6). This describes stabilization mechanisms operating in the substitution positions, which are more effective for R = OCH_3. The values corresponding to Z2 conformers for R = OH are shown in Table S3 (electronic supplementary material).

Analysis of MEP through the NBO-AIM study

MEP maps have been used extensively for predicting the behavior and reactivity of a wide variety of chemical systems [26–33].

The V(r) potentials, created in the space around a molecule by its nuclei and electrons, are a useful tool for the study of molecular reactivity. Unlike other parameters currently used as reactivity indices, V(r) is an actual physical property that can be determined both experimentally and by computational methods. The calculation of physicochemical properties on molecular surface, and its visualization through a color code allows a different view of molecular behavior. This paper uses the procedure proposed by Politzer et al. [26] for predicting sites targeted for electrophilic attack in the regions of negative V(r) values, and NBO and AIM results are reviewed in the light of the complementarity of the different theoretical tools used; thus, a thorough analysis of the role of substituents in the stabilization and reactivity of the structures studied was performed.

In non-substituted species, we found [8] two attack sites that are very close to each other, associated with the O atoms of rings C and E, where the higher values of negative V(r) show that Z1 conformers are more reactive to electrophilic attack, since the negative potential on a group or substructure indicates its tendency to participate in electrostatic interactions, formation of ion pairs or hydrogen bonds. Similar features were observed in substituted species. Upon comparison of negative V(r) values, the following order for reactivity towards electrophilic attack: R = OH < R = H < R = OCH_3 was observed. The values of maximum [V_{max}, positive V(r)], and minimum [V_{min}, negative V(r)] potentials in kcal mol^{-1} are shown in Table 7, (see also Fig. S1a–d in the electronic supplementary material).

Values of V_{min} are higher in Z1 rotamers than in Z2 (Table 7; Fig. S1c, d), which is indicative of the higher

Table 4 Bond polarizations of C-2—C-3 and C-3—C-4 (% at C-2, C-3 and C-4)

Substituent	Conformer	C-2—C-3 bond		C-3—C-4 bond	
R=OH		%C-3	%C-2	%C-4	%C-3
	$Z1_{CT}$	50.77	49.23	49.47	50.53
	$Z1_{CC}$	50.74	49.26	49.43	50.57
	$Z1_{TC}$	50.52	49.48	48.86	51.14
	$Z1_{TT}$	50.56	49.44	48.89	51.11
	$Z2_{CT}$	50.74	49.26	49.81	50.19
	$Z2_{CC}$	50.71	49.29	49.78	50.22
	$Z2_{TC}$	50.56	49.44	49.32	50.68
	$Z2_{TT}$	50.60	49.40	49.36	50.64
R=OCH_3					
	$Z1_{CT}$	50.76	49.24	49.50	50.50
	$Z1_{CC}$	50.73	49.27	49.48	50.52
	$Z2_{CC}$	50.71	49.29	49.83	50.17
R=H					
	Z1	50.65	49.35	49.34	50.66
	Z2	50.63	49.37	49.69	50.31

Table 5 Second-order stabilization energies, $E^{(2)}$, calculated at B3LYP/6-311++G** level of theory for donation and back donation transferences related to R = OCH_3 moiety[a]

$Z1_{CT}$			$Z1_{CC}$			$Z2_{CC}$		
Donor	Acceptor	$E^{(2)}$	Donor	Acceptor	$E^{(2)}$	Donor	Acceptor	$E^{(2)}$
R = OCH_3 (donation transferences)								
σ C-3″—O-3″	σ* C-4″—C-5″	1.51	σ C-3″—O-3″	σ * C-4″—C-5″	1.16	σ C-3″—O-3″	σ * C-4″—C-5″	1.19
	σ * C-2″—C-3″	0.59		σ * C-2″—C-3″	1.45		σ C-2″—C-3″	1.47
	σ* C-1″—C-2″	1.05						
	Σ	**3.15**		**Σ**	**2.61**		**Σ**	**2.66**
σ C-5″—O-5″	σ * C-3″—C-4″	1.10	σ C-5″—O-5″	σ * C-3″—C-4″	1.17	σ C-5″—O-5″	σ * C-3″—C-4″	1.16
	σ * C-4″—C-5″	0.67		σ * C-4″—C-5″	0.64		σ * C-4″—C-5″	0.65
	σ * C-1″—C-6″	1.81		σ* C-1″—C-6″	1.99		σ * C-1″—C-6″	1.90
	σ * C-5″—C-6″	0.65		σ * C-5″—C-6″	0.71		σ* C-5″—C-6″	0.68
	Σ	**4.23**		**Σ**	**4.51**		**Σ**	**4.39**
σ O-3″—C-3a″	σ * C-3″—C-4″	3.11	σ O-3″—C-3a″	σ * C-3″—C-4″	2.93	σ O-3″—C-3a″	σ * C-3″—C-4″	2.91
	Σ	**3.11**		**Σ**	**2.93**		**Σ**	**2.91**
σ O-5″—C-5a″	σ * C-5″—C-6″	2.68	σ O-5″—C-5a″	σ * C-5″—C-6″	2.60	σ O-5″—C-5a″	σ* C-5″—C-6″	2.60
	Σ	**2.68**		**Σ**	**2.60**		**Σ**	**2.60**
1n O-3″	σ * C-2″—C-3″	7.38	1n O-3″	σ* C-3″—C-4″	7.38	1n O-3″	σ* C-3″—C-4″	7.96
	σ *C-3a″—H	0.87		σ * C-2″—C-3″	0.56		σ* C-2″—C-3″	0.56
	σ* C-3a″—H	2.68		σ * C-3a″—H	2.77		σ *C-3a″—H	2.77
	σ* C-3a″—H	0.89		σ * C-3a″—H	0.91		σ * C-3a″—H	0.91
				σ * C-3a″—H	0.92		σ * C-3a″—H	0.92
	Σ	**11.82**		**Σ**	**12.54**		**Σ**	**13.12**
2n O-3″	σ * C-3a″—H	0.89	2n O-3″	π* C-3″—C-4″	30.54	2n O-3″	π * C3″—C-4″	30.50
	π* C-3″—C-4″	28.00		σ * C-3a″—H	5.90		σ* C-3a″—H	5.91
	σ * C-3a″—H	5.76		σ * C3a″—H	5.93		σ* C-3a″—H	5.94
	σ * C-3a″—H	5.79						
	Σ	**40.44**		**Σ**	**55.83**		**Σ**	**56.39**
1n O-5″	σ * C-4″—C-5″	7.13	1n O-5″	σ* C-4″—C-5″	7.23	1n O-5″	σ* C-4″—C-5″	7.30
	σ* C-5″—C-6″	0.68		σ* C-5″—C-6″	0.65		σ* C-5″—C-6″	0.68
	σ * C-5a″—H	2.69		σ* C-5a″—H	0.90		σ* C-5a″—H	0.89
	σ * C-5a″—H	0.87		σ* C-5a″—H	0.82		σ* C-5a″—H	0.82
	σ * C-5a″—H	0.80		σ *C-5a″—H	2.76		σ* C-5a″—H	2.75
	Σ	**12.17**		**Σ**	**12.36**		**Σ**	**12.44**
2n O-5″	π* C-5″—C-6″	26.42	2n O-5″	π* C-5″—C-6″	26.48	2n O-5″	π* C-5″—C-6″	26.45
	σ* C-5a″—H	5.63		σ * C-5a″—H	5.71		σ* C-5a″—H	5.73
	σ* C-5 ″—H	5.76		σ * C-5″—H	5.88		σ* C-5″—H	5.86
	Σ	**37.81**		**Σ**	**38.07**		**Σ**	**38.04**
R = OCH_3 (back donation transferences)								
σ C-4″—C-5″	σ* C-3″—O-3″	3.24	σ C-4″—C-5″	σ* C-3″—O-3″	4.48	σ C-4″—C-5″	σ* C-3″—O-3″	4.47
σ C-4″—H		1.06	σ C-4″—H		0.58	σ C-4″—H		0.58
σ C-1″—C-2″		5.12	σ C-1″—C-2″		3.67	σ C-1″—C-2″		3.68
σ C-2″—H		0.54	σ C-2″—H		1.11	σ C-2″—H		1.11
σ C-3a″—H		3.61	σ C-3a″—H		3.64	σ C-3a″—H		3.64
	Σ	**13.57**		**Σ**	**13.48**		**Σ**	**13.48**
σ C-3″—C-4″	σ* C-5″—O-5″	5.06	σ C-3″—C-4″	σ* C-5″—O-5″	4.68	σ C-3″—C-4″	σ* C-5″—O-5″	4.73
σ C-4″—H		0.74	σ C-4″—H		0.69	σ C-4″—H		0.69
σ C-1″—C-6″		3.44	σ C-1″—C-6″		3.54	σ C-1″—C-6″		3.59
σ C-5a″—H		3.61	σ C-5″—C-6″		0.53	σ C-5″—C-6″		0.55

Table 5 (continued)

$Z1_{CT}$			$Z1_{CC}$			$Z2_{CC}$		
Donor	Acceptor	$E^{(2)}$	Donor	Acceptor	$E^{(2)}$	Donor	Acceptor	$E^{(2)}$
			$\sigma_{C\text{-}5a''—H}$		3.66	$\sigma_{C\text{-}5a''—H}$		3.64
	Σ	**12.85**		**Σ**	**13.1**		**Σ**	**13.2**
$\sigma_{C\text{-}5''—C\text{-}6''}$	$\sigma^*_{O\text{-}5''—C\text{-}5a''}$	3.34	$\sigma_{C\text{-}5''—C\text{-}6''}$	$\sigma^*_{O\text{-}5''—C\text{-}5a''}$	3.4	$\sigma_{C\text{-}5''—C\text{-}6''}$	$\sigma^*_{O\text{-}5''—C\text{-}5a''}$	3.32
$\sigma_{C\text{-}5a''—H}$		0.54	$\sigma_{C\text{-}5a''—H}$		0.53	$\sigma_{C\text{-}5a''—H}$		0.53
$\sigma_{C\text{-}5a''—H}$		0.52	$\sigma_{C\text{-}5a''—H}$		0.50	$\sigma_{C\text{-}5a''—H}$		0.50
	Σ	**4.40**		**Σ**	**4.43**		**Σ**	**4.35**
$\sigma_{C\text{-}3''—C\text{-}4''}$	$\sigma^*_{O\text{-}3''—C\text{-}3a''}$	3.25	$\sigma_{C\text{-}2''—C\text{-}3''}$	$\sigma^*_{O\text{-}3''—C\text{-}3a''}$	3.29	$\sigma_{C\text{-}2''—C\text{-}3''}$	$\sigma^*_{O\text{-}3''—C\text{-}3a''}$	3.30
$\sigma_{C\text{-}3a''—H}$		0.53	$\sigma_{C\text{-}3a''—H}$		0.53	$\sigma_{C\text{-}3a''—H}$		0.53
$\sigma_{C\text{-}3a''—H}$		0.54	$\sigma_{C\text{-}3a''—H}$		0.53	$\sigma_{C\text{-}3a''—H}$		0.53
	Σ	**4.32**		**Σ**	**4.35**		**Σ**	**4.36**

[a] All values are expressed in kcal mol^{-1}

inductive effect exerted by the O and O1 oxygen atoms in the most stable rotamers (Z1) [8].

The percentage values of electron density on each atom of C-1′—C-6′ and C-1′—C-2′ bonds by NBO calculations are shown in Table 8. As already stated, the difference between the values found on each atom of a bond quantifies the polarization or ionicity thereof. Therefore, C-1′—C-6′ and C-1′—C-2′ bonds are more polarized in Z1 rotamers than in Z2, which indicates a higher inductive effect in Z1 than in Z2 for all substituents. Interestingly, the highest polarization found in C-1′—C-6′ and C-1′—C-2′ bonds correlates with a greater electron delocalization in Z1 conformers than in Z2, which is related to hyperconjugative interactions between O-1—C-2 and O1—C-8a bonds (and those of the symmetrically equivalent bonds: O—C-2 and O—C1″) with adjacent bonds that connect the γ-pyran substructure with ring B: C-2—C-1′, C-1′—C-2′ and C-1′—C-6′. These interactions in Z1 are up to 24% more intense than in Z2 conformers, thus determining its higher stabilization.

When we related the major intensity of the hyperconjugative effects mentioned above with the highest polarization of C-1′—C-6′ and C-1′—C-2′ bonds, we found in all structures an inductive effect exerted by O and O1 atoms assisted by resonance, which reaches a maximum intensity when each structure has the highest stabilization.

The plane of the molecule (ring A, and part of ring C) divides the space into two regions: one above this plane, and another below it. In Z1 rotamers, ring B has one side towards the upper part of the molecule (“upper side of B”), and the other towards the lower part of the molecule (“lower side of B”). Regardless of the substitution, a remarkable difference in *V*(r) distribution is observed in these two sides, a higher negative potential expansion being found on the second side due to the proximity of the O-1—C-O active site (Fig. 5a,b).

For R = OH, the negative *V*(r) on the O attached to C-3″ ("the outside one") is higher than that of the O attached to C-5″ [$\Delta_{O\text{-}3''\text{-}O\text{-}5''}$: (−58.82) − (−43.35) = −15.47 kcal mol^{-1} for $Z1_{TC,}$] (Figs. 5a,b). Consequently, the respective NCP charge density follows this trend, leading to an electron density on O-3″ of 295.210 a.u. for Z1 and 295.211 for Z2, and on O-5″ 295.203 a.u. for Z1 and 295.197 a.u. for Z2.

It is also possible to relate *V*(r) to the increase in CP electron density of the C-3″—O bond, which is 0.284 a.u. (on average, considering Z1 and Z2 conformers) while the mean value for C–5″—O is 0.281 a.u.

The O attached to C-5″ has a lower negative *V*(r) in “C” (−43.3 kcal mol^{-1}) than that in “T” disposition (−58.98 kcal mol^{-1}; Fig. 5c,d), its electron density in NCP is also lower (295.195 a.u. and 295.204 a.u., respectively), and consequently the electron density in CP of the C-5′′—O bond (Table S1).

V(r) values for R = OCH_3 are also more negative on the O attached to C-3″ (“the outside one”) than that attached to C-5″ [$\Delta_{O\text{-}3''\text{-}O\text{-}5''}$: (−64.89) − (−52.93) = − 11.96 kcal mol^{-1}]. For any of these positions, more negative potentials (mean difference of 6.13 kcal mol^{-1}) are always found than on the oxygen atoms of the R = OH substituent (see Fig. 6a,b). For all conformers with R = OCH_3, the mean electron density in BCP is also higher on C-3″—O (0.28302 a.u.) than on C-5″—O (0.27993 a.u.), in agreement with the findings for R = OH. Similarly, NCP electron density is 295.188 a.u. on C-3″, and 295.172 a.u. on C-5″, as mean values for Z1 and Z2.

Electron donation (transfers that remove charge from the bond) and electron back-donation (reverse charge transfers towards the bond) related to C-3″—O and C-5″—O bonds show that the difference between both contributions is negative and large in the former case, thus explaining the higher intensity of negative *V*(r) on O-3″ than on O-5″ (Tables 5, 6). Using the same arguments, it is also possible

Table 6 Second-order stabilization energies, $E^{(2)}$, calculated at B3LYP/6-311++G** level of theory, for donation and back donation transferences related to R = OH moiety in Z1 conformers[a]

$Z1_{CT}$			$Z1_{CC}$			$Z1_{TC}$			$Z1_{TT}$		
Donor	Acceptor	$E^{(2)}$	Donor	Acceptor	$E^{(2)}$	Donor	Acceptor	$E^{(2)}$	Donor	Acceptor	$E^{(2)}$
R=OH (donation transferences)											
$\sigma_{C\text{-}3''—O\text{-}3''}$	$\sigma^*_{C\text{-}4''—C\text{-}5''}$	7.13	$\sigma_{C\text{-}3''—O\text{-}3''}$	$\sigma^*_{C\text{-}3''—C\text{-}4''}$	0.54	$\sigma_{C\text{-}3''—O\text{-}3''}$	$\sigma^*_{C\text{-}3''—C\text{-}4''}$	0.55	$\sigma_{C\text{-}3''—O\text{-}3''}$	$\sigma^*_{C\text{-}4''—C\text{-}5''}$	1.35
	$\sigma^*_{C\text{-}2''—C\text{-}3''}$	0.59		$\sigma^*_{C\text{-}2''—C\text{-}3''}$	1.19		$\sigma^*_{C\text{-}2''—C\text{-}3''}$	1.18		$\sigma^*_{C\text{-}2''—C\text{-}3''}$	0.63
	$\sigma^*_{C\text{-}1''—C\text{-}2''}$	1.29		$\sigma^*_{C\text{-}1''—C\text{-}2''}$	1.49		$\sigma^*_{C\text{-}1''—C\text{-}2''}$	1.38		$\sigma^*_{C\text{-}1''—C\text{-}2''}$	1.23
	Σ	**3.25**		**Σ**	**3.22**		**Σ**	**3.11**		**Σ**	**3.21**
$\sigma_{C\text{-}5''—O\text{-}5''}$	$\sigma^*_{C\text{-}3''—C\text{-}4''}$	1.15	$\sigma_{C\text{-}5''—O\text{-}5''}$	$\sigma^*_{C\text{-}3''—C\text{-}4''}$	1.16	$\sigma_{C\text{-}5''—O\text{-}5''}$	$\sigma^*_{C\text{-}3''—C\text{-}4''}$	1.45	$\sigma_{C\text{-}5''—O\text{-}5''}$	$\sigma^*_{C\text{-}3''—C\text{-}4''}$	1.41
	$\sigma^*_{C\text{-}4''—C\text{-}5''}$	0.66		$\sigma^*_{C\text{-}4''—C\text{-}5''}$	0.67		$\sigma^*_{C\text{-}1''—C\text{-}6''}$	1.73		$\sigma^*_{C\text{-}1''—C\text{-}6''}$	1.62
	$\sigma^*_{C\text{-}1''—C\text{-}6''}$	2.15		$\sigma^*_{C\text{-}1''—C\text{-}6''}$	1.98		$\sigma^*_{C\text{-}5''—C\text{-}6''}$	0.75		$\sigma^*_{C\text{-}5''—C\text{-}6''}$	0.69
	$\sigma^*_{C\text{-}5''—C\text{-}6''}$	0.79		$\sigma^*_{C\text{-}5''—C\text{-}6''}$	0.77						
	Σ	**4.75**		**Σ**	**4.58**		**Σ**	**3.93**		**Σ**	**3.72**
$\sigma_{O\text{-}3''—H}$	$\sigma^*_{C\text{-}3''—C\text{-}4''}$	5.15	$\sigma_{O\text{-}3''—H}$	$\sigma^*_{C\text{-}2''—C\text{-}3''}$	4.98	$\sigma_{O\text{-}3''—H}$	$\sigma^*_{C\text{-}2''—C\text{-}3''}$	4.79	$\sigma_{O\text{-}3''—H}$	$\sigma^*_{C\text{-}3''—C\text{-}4''}$	5.02
	Σ	**5.15**		**Σ**	**4.98**		**Σ**	**4.79**		**Σ**	**5.02**
$\sigma_{O\text{-}5''—H}$	$\sigma^*_{C\text{-}5''—C\text{-}6''}$	4.40	$\sigma_{O\text{-}5''—H}$	$\sigma^*_{C\text{-}5''—C\text{-}6''}$	4.39	$\sigma_{O\text{-}5''—H}$	$\sigma^*_{C\text{-}4''—C\text{-}5''}$	4.81	$\sigma_{O\text{-}5''—H}$	$\sigma^*_{C\text{-}4''—C\text{-}5''}$	4.71
	Σ	**4.40**		**Σ**	**4.39**		**Σ**	**4.81**		**Σ**	**4.71**
$1n_{O\text{-}3''}$	$\sigma^*_{C\text{-}2''—C\text{-}3''}$	6.76	$1n_{O\text{-}3''}$	$\sigma^*_{C\text{-}3''—C\text{-}4''}$	6.87	$1n_{O\text{-}3''}$	$\sigma^*_{C\text{-}3''—C\text{-}4''}$	6.80	$1n_{O\text{-}3''}$	$\sigma^*_{C\text{-}2''—C\text{-}3''}$	6.62
	Σ	**6.76**		**Σ**	**6.87**		**Σ**	**6.80**		**Σ**	**6.62**
$2n_{O\text{-}3''}$	$\pi^*_{C\text{-}3''—C\text{-}4''}$	28.17	$2n_{O\text{-}3''}$	$\pi^*_{C\text{-}3''—C\text{-}4''}$	29.12	$2n_{O\text{-}3''}$	$\pi^*_{C\text{-}3''—C\text{-}4''}$	28.89	$2n_{O\text{-}3''}$	$\pi^*_{C\text{-}3''—C\text{-}4''}$	27.87
	Σ	**28.17**		**Σ**	**29.12**		**Σ**	**28.89**		**Σ**	**27.87**
$1n_{O\text{-}5''}$	$\sigma^*_{C\text{-}4''—C\text{-}5''}$	6.08	$1n_{O\text{-}5''}$	$\sigma^*_{C\text{-}4''—C\text{-}5''}$	6.21	$1n_{O\text{-}5''}$	$\sigma^*_{C\text{-}4''—C\text{-}5''}$	6.81	$1n_{O\text{-}5''}$	$\sigma^*_{C\text{-}4''—C\text{-}5''}$	6.82
	Σ	**6.08**		**Σ**	**6.21**		**Σ**	**6.81**		**Σ**	**6.82**
$2n_{O\text{-}5''}$	$\pi^*_{C\text{-}5''—C\text{-}6''}$	26.50	$2n_{O\text{-}5''}$	$\pi^*_{C\text{-}5''—C\text{-}6''}$	26.33	$2n_{O\text{-}5''}$	$\pi^*_{C\text{-}5''—C\text{-}6''}$	27.97	$2n_{O\text{-}5''}$	$\pi^*_{C\text{-}5''—C\text{-}6''}$	28.09
	Σ	**26.50**		**Σ**	**26.33**		**Σ**	**27.97**		**Σ**	**28.09**
R=OH (back donation transferences)											
$\sigma_{C\text{-}4''—C\text{-}5''}$	$\sigma^*_{C\text{-}3''—O\text{-}3''}$	3.71	$\sigma_{C\text{-}4''—C\text{-}5''}$	$\sigma^*_{C\text{-}3''—O\text{-}3''}$	4.29	$\sigma_{C\text{-}4''—C\text{-}5''}$	$\sigma^*_{C\text{-}3''—O\text{-}3''}$	4.34	$\sigma_{C\text{-}4''—C\text{-}5''}$	$\sigma^*_{C\text{-}3''—O\text{-}3''}$	3.78
$\sigma_{C\text{-}4''—H}$		0.78	$\sigma_{C\text{-}4''—H}$		0.61	$\sigma_{C\text{-}4''—H}$		0.67	$\sigma_{C\text{-}4''—H}$		0.81
$\sigma_{C\text{-}1''—C\text{-}2''}$		4.57	$\sigma_{C\text{-}1''—C\text{-}2''}$		4.02	$\sigma_{C\text{-}1''—C\text{-}2''}$		3.92	$\sigma_{C\text{-}1''—C\text{-}2''}$		4.62
$\sigma_{C\text{-}2''—H}$		0.67	$\sigma_{C\text{-}2''—H}$		0.82	$\sigma_{C\text{-}2''—H}$		0.76	$\sigma_{C\text{-}2''—H}$		0.61
	Σ	**9.73**		**Σ**	**9.74**		**Σ**	**9.69**		**Σ**	**9.82**
$\sigma_{C\text{-}3''—C\text{-}4''}$	$\sigma^*_{C\text{-}5''—O\text{-}5''}$	4.67	$\sigma_{C\text{-}3''—C\text{-}4''}$	$\sigma^*_{C\text{-}5''—O\text{-}5''}$	4.56	$\sigma_{C\text{-}3''—C\text{-}4''}$	$\sigma^*_{C\text{-}5''—O\text{-}5''}$	3.72	$\sigma_{C\text{-}3''—C\text{-}4''}$	$\sigma^*_{C\text{-}5''—O\text{-}5''}$	3.89
$\sigma_{C\text{-}4''H}$		0.74	$\sigma_{C\text{-}4''—H}$		0.69	$\sigma_{C\text{-}4''—H}$		0.85	$\sigma_{C\text{-}4''—H}$		0.90
$\sigma_{C\text{-}1''—C\text{-}6''}$		3.88	$\sigma_{C\text{-}1''—C\text{-}6''}$		3.84	$\sigma_{C\text{-}1''—C\text{-}6''}$		4.43	$\sigma_{C\text{-}1''—C\text{-}6''}$		4.20
	Σ	**9.29**		**Σ**	**9.09**		**Σ**	**9.00**		**Σ**	**8.99**
$\sigma_{C\text{-}3''—C\text{-}4''}$	$\sigma^*_{O\text{-}3''—H}$	1.76	$\sigma_{C\text{-}3''—C\text{-}4''}$	$\sigma^*_{O\text{-}3''—H}$	1.78	$\sigma_{C\text{-}2''—C\text{-}3''}$	$\sigma^*_{O\text{-}3''—H}$	1.74	$\sigma_{C\text{-}2''—C\text{-}3''}$	$\sigma^*_{O\text{-}3''—H}$	1.76
	Σ	**1.76**		**Σ**	**1.78**		**Σ**	**1.74**		**Σ**	**1.76**
$\sigma_{C\text{-}5''—C\text{-}6''}$	$\sigma^*_{O\text{-}5''—H}$	1.60	$\sigma_{C\text{-}5''—C\text{-}6''}$	$\sigma^*_{O\text{-}5''—H}$	1.62	$\sigma_{C\text{-}5''—C\text{-}6''}$	$\sigma^*_{O\text{-}5''—H}$	1.80	$\sigma_{C\text{-}5''—C\text{-}6''}$	$\sigma^*_{O\text{-}5''—H}$	1.83
						$\sigma_{C\text{-}4—H}$		0.52	$\sigma_{C\text{-}4—H}$		0.52
	Σ	**1.60**		**Σ**	**1.62**		**Σ**	**2.32**		**Σ**	**2.35**

[a] All values are expressed in kcal mol^{-1}

to justify the higher intensity of negative $V(r)$ of the oxygen atoms of OCH_3 groups with respect to the potential on oxygen atoms of OH groups, as has been observed in the MEPs mentioned above.

All this suggests a higher reactivity of the substituent at C-3″, and explains the mechanisms underlying this condition. The substituent at C-5″ operates in hydrogen bond-type interactions in all structures, as described above.

Hyperconjugative interactions related to R = OCH_3 and R = OH substituents are shown in Tables 5 and 6, respectively. From these tables it is possible to delve deeper into the study of the role of substituents in the structures of

A-type proanthocyanidins. Thus, it is shown that all bonds are better acceptors than donors, i.e., transfers that take charge to antibonding orbitals are more important than those that remove charge from bonding orbitals. The exception is the OH bond, which is a much better donor than acceptor (cf. transfer energies that take charge to it with those from it; Table 6, S3). Therefore, since only part of the OH electron delivery comes from hyperconjugative delocalizations (OH donates more than it receives by hyperconjugation) it is postulated that, by charge conservation, the remaining charge delivered comes from the charge concentration in the area associated with the higher EW (electron withdrawing) effect of O-5″—H and O-3″—H, e.g., from the σ cloud via inductive effects. From NBO analysis, this mechanism then describes the major EW effect of OH against the OCH_3 group. Although the electron donor ability of a CH_3 towards a closed π-system is known, the occurrence of the methoxyl oxygen atom prevents donations from CH_3 reaching the aromatic ring, thus showing the EW effect of the oxygen of the adjacent C—O bond (Table 5).

The occurrence of an inductive effect assisted by resonance has been reported for O-O1 atoms [8]. Concerning the oxygen atoms of substituents, as mentioned above, the associated resonance mechanisms are higher for R = OH, and a higher inductive effect can also be postulated in agreement with that mentioned above, due to the high O-H donor capacity.

This high donor capacity is also evidenced by MEP analysis. The difference in electrostatic potential values on the various hydrogens is remarkable. Those of the OH group have always a higher positive value (72.79 kcal mol^{-1}) regardless of the conformer, thus indicating the high donor role of this group (Fig. 6b). The increase in positive $V(r)$ on the hydrogen atoms of the C-3—H2 group (Fig. 7c, oblique lines) can be similarly explained. The donor role of these C—H bonds in hyperconjugative interactions has been related to their weakening and elongation [8].

Upon analysis of the hydrogen atoms of the OCH_3 group, we found that those attached to C-5″ in the "C"-type position showed an extended area of higher positive $V(r)$ value (34.05 kcal mol^{-1}), covering the three hydrogen atoms. Similar results were observed for the hydrogen atoms attached to C-3″ in "C". However, when this substituent adopted the "T" configuration, the area of positive potential was reduced, being concentrated only on each individual hydrogen atom (Fig. 7). Again, these results have a counterpart in the donor role of the related C–H bonds. In fact, by NBO analysis (Table 5), the increase in positive potential in "C" dispositions was explained by taking into account the increase in C–H donor capacity (and/or increase in the acceptor ability of the C-3″—O-3″ bond) in this configuration with respect to the donor ability in the "T" configuration (the energy associated with $\sigma_{C\text{-}3a''—H} \rightarrow \sigma^*_{C\text{-}2—O\text{-}3''}$ transfer is 3.64 kcal mol^{-1} for "T", and 3.61 kcal mol^{-1} for "C"). Therefore, a higher loss of charge on hydrogen atoms is expected in "C" than in "T".

The $V(r)$ values on oxygen atoms that comprise a hydrogen bond (atom of the acceptor moiety) become less negative (higher) than $V(r)$ of those that do not comprise it ($\Delta_{O\text{-}3''\text{-}O\text{-}5''}$ = 15.46 kcal mol^{-1} for $Z1_{CC}$ conformers with R = OH).

Table 7 Ranges of $V(r)$ potentials (kcal mol^{-1})

Substituent	Conformer	V_{max}	V_{min}
OH			
	$Z1_{CT}$	72.60	–79.33
	$Z1_{CC}$	72.27	–79.62
	$Z1_{TC}$	70.99	–76.68
	$Z1_{TT}$	72.65	–76.46
	$Z2_{CT}$	70.85	–76.41
	$Z2_{CC}$	70.56	–76.45
	$Z2_{TC}$	68.68	–72.76
	$Z2_{TT}$	67.61	–73.10
OCH_3			
	$Z1_{CT}$	35.48	–83.00
	$Z1_{CC}$	37.76	–84.85
	$Z2_{CC}$	37.03	–80.63
H			
	Z1	27.48	–82.01
	Z2	28.05	–78.83

Table 8 Bond polarizations of C-1′—C-2′ and C-1′—C-6′, % at C-1′, C-2′ and C-6′

Substituent	Conformer	C-1′—C-2′ bond		C-1′—C-6′ bond	
OH		% C-2′	% C-1′	% C-6′	% C-1′
	$Z1_{CT}$	51.08	48.92	51.39	48.61
	$Z1_{CC}$	51.07	48.93	51.46	48.54
	$Z1_{TC}$	51.12	48.93	51.07	48.88
	$Z1_{TT}$	51.10	48.91	51.09	48.90
	$Z2_{CT}$	50.72	49.28	50.67	49.33
	$Z2_{CC}$	50.73	49.27	50.44	49.56
	$Z2_{TC}$	50.77	49.23	50.75	49.25
	$Z2_{TT}$	50.47	49.25	50.75	49.53
OCH_3					
	$Z1_{CT}$	51.06	48.94	51.34	48.66
	$Z1_{CC}$	51.05	48.95	51.41	48.59
	$Z2_{CC}$	50.72	49.28	50.42	49.58
H					
	Z1	51.08	48.92	51.08	48.92
	Z2	50.74	49.26	50.44	49.56

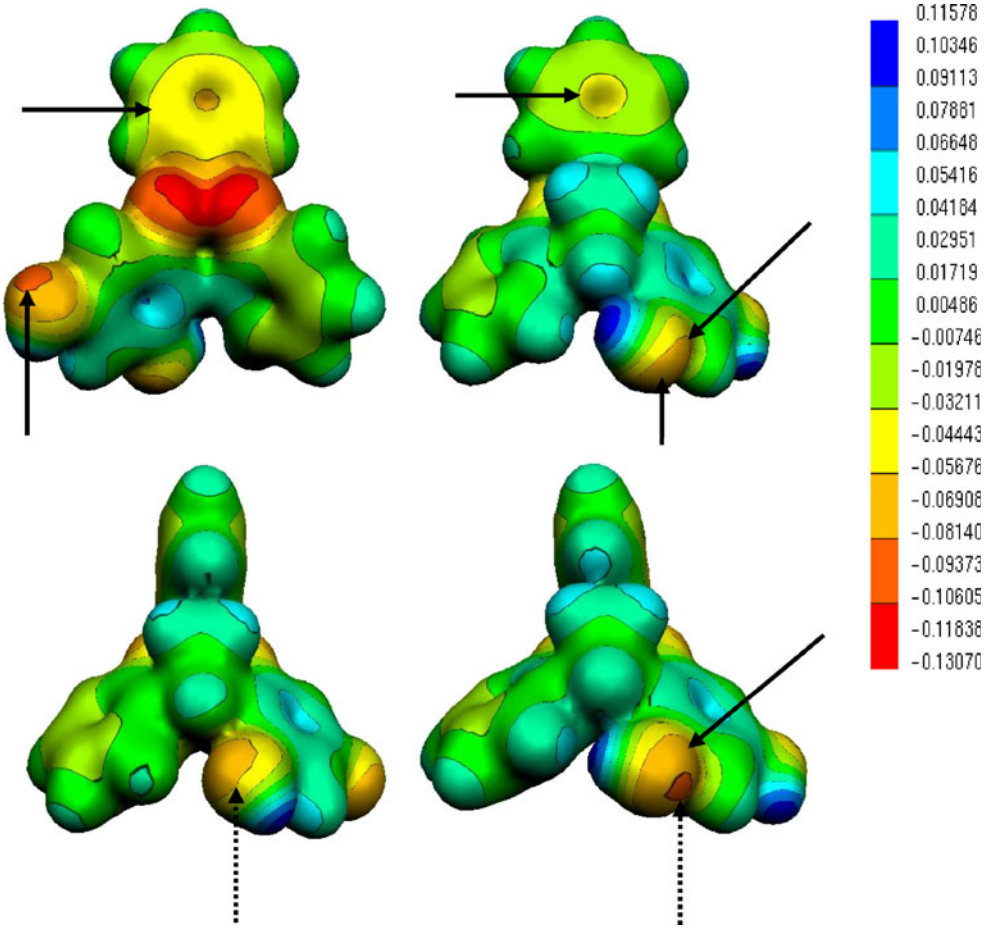

Fig. 5 Maps of molecular electrostatic potential (MEP) for $Z1_{TC}$ conformers of A-type dimeric proanthocyanidin substituted with R = OH (in a.u.). The upper (**a**) and lower (**b**) sides of ring B are shown (see text for definitions). (**c**) Rotamer ($Z2_{CT}$). *Horizontal lines* indicate the spreading of negative potential at the lower side of ring B. *Vertical lines* indicate the differences in V(r) over oxygen atoms of substituents. *Oblique lines* indicate the differences of V(r) at O-5″ in Z1 (**b**) and in Z2 (**c**). *Dashed lines* indicate changes in V(r) at O-5″ for type "C"(**c**) and "T" (**d**) arrangements

The positive V(r) values on hydrogens of the O···H hydrogen bridge (belonging to the donor C–H moiety) become more negative (lower) than the other H of the benzene ring (Figs. 5c, 6a–c, 7c), i.e., in $Z1_{CC}$ for R = OCH_3 $\Delta_{H\neq5\text{-}H5}$=18.52−3.05 kcal mol^{-1}=15.47 kcal mol^{-1}. Thus, MEP analysis suggests the formation of intramolecular H···O hydrogen bonds. The V(r) value on the atom that belongs to the acceptor moiety increases, while the V(r)

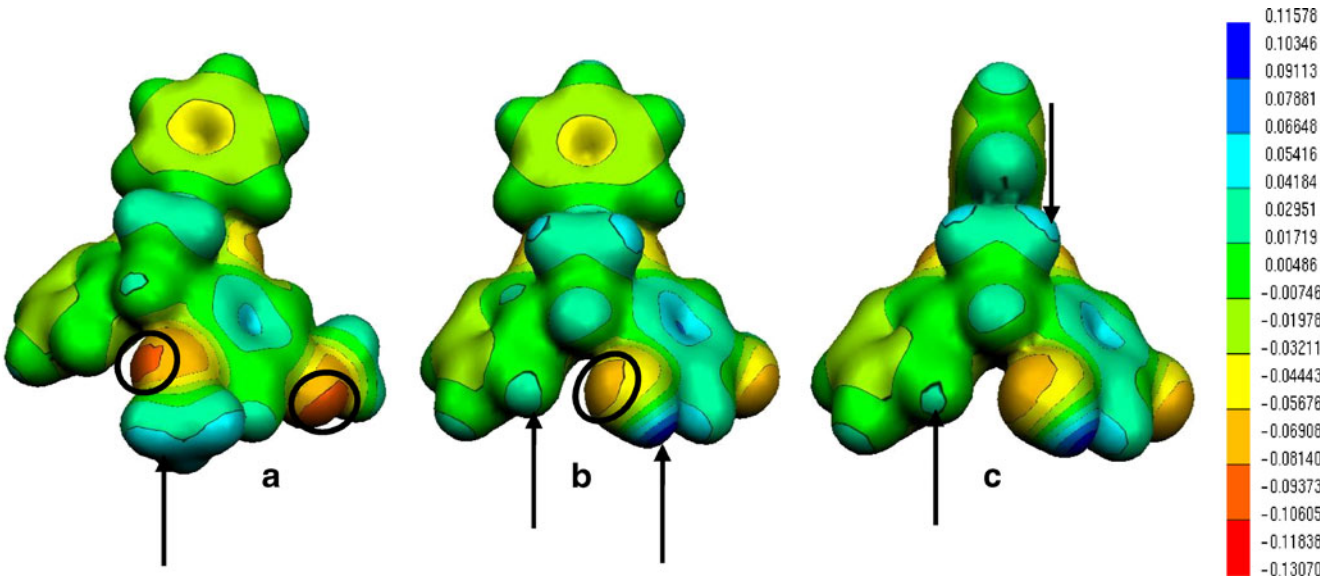

Fig. 6 Maps of MEP for $Z1_{CT}$ conformers of A-type dimeric proanthocyanidins substituted with R = OCH_3 (**a**) and R = OH (**b**) (in a.u.). Circles in (**a**) and (**b**) indicate differences between V(r) at oxygen atoms of OCH_3 and OH moieties. $Z2_{CT}$ rotamer with R = OH is also shown (**c**). *Vertical lines* indicate different behavior of V(r) at hydrogen atoms

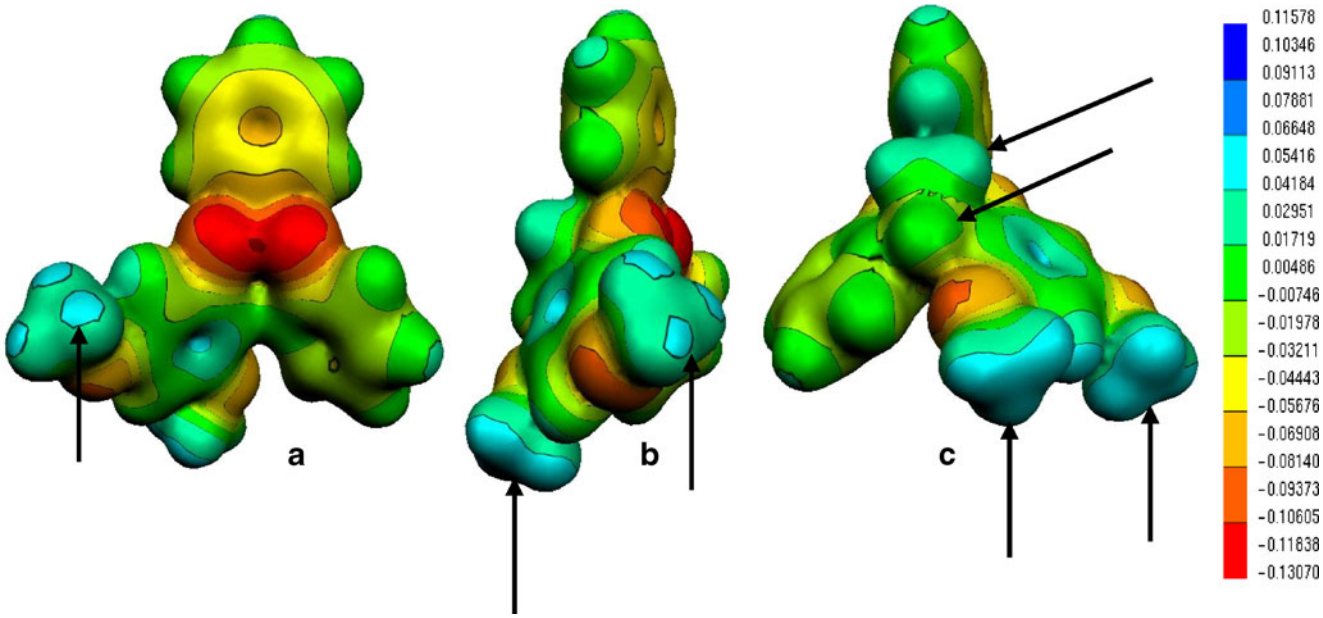

Fig. 7 Maps of MEP for $Z1_{CT}$ (**a**, **b**) and $Z2_{CC}$ (**c**) conformers of A-type dimeric proanthocyanidin substituted with R = OCH_3 (in a.u.). *Oblique lines* indicate the increase of *V*(r) at hydrogen atoms of the C-3H2 moiety. *Vertical lines* indicate different behavior of *V*(r) at hydrogen atoms of the R = OCH_3 substituent

value decreases on that of the donor moiety. These results are in agreement with the electrostatic potential complementarity between positive regions of H-donor groups and negative regions of the H-acceptor atom found in intermolecular H-bonds [18].

MEPs and NBO analyses highlight another topic, i.e., the possibility of characterizing the electrostatic nature of both H···O and H···H intramolecular weak interactions, and their marked directionality. The latter is visible when realizing the asymmetry of the *V*(r) distribution of hydrogen and oxygen atoms of the bridge, which is defined clearly by the neighbor oxygen and hydrogen positions (Figs. 5b, d, 6a and 7c).

Conclusions

We carried out a study of the stereochemistry of dimeric proanthocyanidins, highlighting description of the factors that determine stereochemistry, and the changes that occur with R = OCH_3, R′ = H, and R = OH, R′ = H as substituents, starting with a study of the conformational space of each species. Two conformers of lowest energy were characterized for R = H, eight conformers for R = OH, and three conformers for R = OCH_3.

Intramolecular interactions were studied and characterized by AIM theory, analyzing the common features for all structures. In all substituted structures, BCPs were also found to define intramolecular weak hydrogen bond-type interactions. Some had intramolecular conventional bridges, while others had intramolecular dihydrogen-type non-conventional interactions. These interactions have been the focus of much recent research, and their discovery in organic compounds is of high interest.

Specifically, at the B3LYP/6-311++G** level of calculation, the following intermolecular hydrogen bond interactions were characterized: (1) H···O type (in $Z1_{CT}$, $Z1_{CC}$, $Z2_{CT}$ and $Z2_{CC}$ conformers for R = OH, and in all conformers for R = OCH_3), and (2) dihydrogen-type, such as C-5—H-5···H-5″—O5″ and C-4—H-4···H-5″—O5″ (in $Z1_{TC}$ and $Z1_{TT}$, R = OH), and C-5—H-5···H-5″ (in $Z2_{TC}$ and $Z2_{TT}$, R = OH).

Through a detailed NBO analysis, subtle stereoelectronic aspects of fundamental importance to the understanding the stabilization and antioxidant function of these structures were described. We described the resonance of the lone pairs of both O and O1 oxygens and concluded that substitution gives rise to a C-2—C-3 bond that is more polarized than C-3—C-4, and that polarization increases in the order R = H < R = OCH_3 < R = OH. Furthermore, we showed that conformational changes are correlated with the relative structure stability through the hyperconjugative mechanisms described above. Stabilization mechanisms were also described in the substitution positions, being more effective when R = OCH_3.

This study was enriched by a deep analysis of MEP maps, which are used for predicting sites targeted for electrophilic attack in the negative *V*(r) regions, and also for rationalizing other aspects of their distribution in the light of the complementarity of the different theoretical tools used herein.

All species had two, closely spaced attack sites associated with the oxygen atoms of rings C and E, where higher negative $V(r)$ values show that Z1 conformers are more reactive for electrophilic attack. Accordingly, it was concluded that C-1′—C-2′ and C-1′—C-6′ bonds are more polarized in Z1 than in Z2, thus correlating with the higher intensity of hyperconjugative interactions between them and those oxygen atoms. This in turn leads to the conclusion that an inductive effect, assisted by resonance, is exerted by both O and O1 atoms, which reaches maximal intensity when each structure has the highest stabilization.

As for the substituted ring, the major reactivity of the substituent group was found at C-3″, and thus mechanisms supporting this condition can be explained. It was also established that the substituent at C-5″ exhibits hydrogen bond-type intramolecular interactions in all structures.

The possibility of distinguishing hydrogen atoms from each other according to the donor role of the bond to which they belong is also noteworthy. Similarly for oxygens, showing that the more important their donor role according to NBO analysis, the more their negative potential will decrease in absolute values.

In addition, we have shown that, in proanthocyanidins, MEP analysis allows the formation of H···O intramolecular hydrogen bonds to be suggested. Another aspect that must be highlighted is the possibility of characterizing both H···O and H···H intramolecular interactions found as weak electrostatic interactions, and to appreciate their remarkable directionality. This is of great interest, primarily in the study of non-conventional-type interactions like dihydrogen bonds, whose nature is still under discussion. The study of the effect of solvent and level of calculation on such interactions is in progress in our laboratory.

This work deepens the analysis of the stereochemistry of dimeric proanthocyanidins, describing hyperconjugative and conjugative effects associated with substituents, and the effect thereof on structure. This analysis aimed to describe a posteriori the stabilization and possible interactions with other organic molecules in a food matrix, thus enabling and validating useful analysis tools to be implemented in subsequent studies of more complex structures. Owing to the unique structural features of proanthocyanidins (presence of two prochiral carbons, and a [3.1.3]-bicyclic rigid substructure), this work represents a major step in the process towards the final study of polymeric species.

Acknowledgments Thanks are due to Agencia de Promoción Científica y Tecnológica Argentina (MINCYT), CONICET, Universidad Nacional de La Plata and Universidad de Buenos Aires (Argentina) for financial support. A.B.P. is a Senior Research Member of the National Research Council of Argentina (CONICET). A.H.J. is Member of the Scientific Research Career (CIC, Provincia de Buenos Aires). E.N.B. acknowledges a fellowship (IP-PRH No 54) from Agencia de Promoción Científica y Tecnológica Argentina and Universidad de la Cuenca del Plata (Corrientes, Argentina). R.M.L. acknowledges Universidad de la Cuenca del Plata for facilities provided during the course of this work.

References

1. Pomilio A, Müller O, Schilling G, Weinges K (1977) Zur Kenntnis der Proanthocyanidine, XXII. Über die Konstitution der Kondensationsprodukte von Phenolen mit Flavyliumsalzen. Justus Liebigs Ann Chem :597-601
2. Ricardo da Silva JM, Darmon N, Fernandez Y, Mitjavilla S (1991) Oxygen free radical scavenger capacity in aqueous models of different procyanidins from grape seeds. J Agric Food Chem 39:1549–1552
3. Liu ZQ, Ma LP, Zhou B, Yang L, Liu ZL (2000) Antioxidative effects of green tea polyphenols on free radical initiated and photosensitized peroxidation of human low density lipoprotein. Chem Phys Lipids 106:53–63
4. Liu L, Xie B, Cao S, Yang E, Xu X, Guo S (2007) A-type procyanidins from *Litchi chinensis* pericarp with antioxidant activity. Food Chem 105:1446–1451
5. Kedage VV, Tilak JC, Dixit GB, Devasagayam TPA, Mhatre M (2007) A study of antioxidantproperties of some varieties of grapes (*Vitis vinifera* L). Crit Rev Food Sci Nutr 47:175–185
6. Pinent M, Bladé C, Salvadó MJ, Blay M, Pujadas G, Fernandez-Larrea J, Arola L, Ardevol A (2006) Procyanidin effects on adipocyte-related pathologies. Crit Rev Food Sci Nutr 46:543–550
7. Pomilio A, Ellmann B, Künstler K, Schilling G, Weinges K (1977) Naturstoffe aus Arzneipflanzen, XXI. ^{13}C-NMR-spektroskopische Untersuchungen an Flavanoiden. Justus Liebigs Ann Chem :588–596
8. Lobayan RM, Jubert AH, Pomilio AB (2009) Conformational and electronic (AIM/NBO) study of unsubstituted A-type dimeric Proanthocyanidin. J Mol Model 15:537–550
9. HyperChem Release 7.5, Hypercube Inc, Gainsville, FL
10. Kudin KN, Strain MC, Farkas O, Tomasi J, Barone V, Cossi M, Cammi R, Mennucci B, Pomelli C, Adamo C, Clifford S, Ochterski J, Petersson GA, Ayala PY, Cui Q, Morokuma K, Malick DK, Rabuck AD, Raghavachari K, Foresman JB, Cioslowski J, Ortiz JV, Baboul AG, Stefanov BB, Liu G, Liashenko A, Piskorz P, Komaromi I, Gomperts R, Martin RL, Fox DJ, Keith T, Al-Laham MA, Peng CY, Nanayakkara A, Gonzalez C, Challacombe M, Gill PMW, Johnson B, Chen W, Wong MW, Andres JL, Gonzalez C, Head-Gordon M, Replogle ES, Pople JA (1998) Gaussian 98, Revision A.7. Gaussian Inc, Pittsburgh
11. Flúkiger P, Lúthi HP, Portmann S, Weber J (2000) MOLEKEL 4.0. Swiss Center for Scientific Computing, Manno, Switzerland
12. Biegler-Koning FW, Bader RFW, Tang TH (1982) Calculation of the average properties of atoms in molecules.II. J Comput Chem 3:317–328
13. Glendening ED, Reed AE, Carpenter JE, Weinhold F NBO 3.1. Program as implemented in the Gaussian 98 package
14. Bader RFW (1995) Atoms in molecules—a quantum theory. Oxford University Press, Oxford
15. Bader RFW (1990) A quantum theory of molecular structure and its applications. Chem Rev 91:893–928
16. Bader RFW (1998) A Bond Path: a universal indicator of bonded interactions. J Phys Chem A 102:7314–7323
17. Popelier PLA (1998) Characterization of a dihydrogen bond on the basis of the electron density. J Phys Chem A 102:1873–1878

18. Carroll MT, Bader RFW (1988) An analysis of the hydrogen bond in BASE-HF complexes using the theory of atoms in molecules. Mol Phys 65:695–722
19. Desiraju GR, Steiner T (1999) The weak hydrogen bond in structural chemistry and biology. Oxford University Press, New York
20. Koch U, Popelier PLA (1995) Characterization of C–H–O hydrogen bonds on the basis of the charge density. J Phys Chem 99:9747–9754
21. Lee JC, Peris E, Rheingod AL, Crabtree CH (1994) An unusual type of H···H interaction: Ir-H···H-O and Ir-H···H–N hydrogen bonding and its involvement in sigma-bond metathesis. J Am Chem Soc 116:11014–11019
22. Pakiari AH, Mohajeri A (2003) Multi dihydrogen bonds. J Mol Struct Theochem 620:31–36
23. Grabowski SJ, Sokalski WA, Leszczynski J (2007) Wide spectrum of H···H interactions; van der Waals contacts, dihydrogen bonds and covalency. Chem Phys 337:68–76
24. Matta CF (2006) The non-electrostatic limit of closed-shell interaction between two hydrogen atoms. A critical review. In: Grabowski SJ (ed) Hydrogen bonding–new insights. Springer, Netherlands, pp 337–375
25. Pacios LF (2006) Changes of electron properties in the formation of hydrogen bonds. In: Grabowski SJ (ed) Hydrogen bonding–new insights. Springer, Netherlands, pp 109–148
26. Politzer P, Truhlar DG (eds) (1981) Chemical applications of atomic and molecular electrostatic potentials. Plenum, NY
27. Politzer P, Landry SJ, Warnheim T (1982) Proposed procedure for using electrostatic potentials to predict and interpret nucleophilic processes. J Phys Chem 86:4767–4771
28. Politzer P, Abrahmsen L, Sjoberg P (1984) Effects of amino and nitro substituents upon the electrostatic potential of an aromatic ring. J Am Chem Soc 106:855–860
29. Politzer P, Laurence PR, Jayasuriya K (1985) Molecular electrostatic potentials: an effective tool for the elucidation of biochemical phenomena. Environ Health Perspect 61:191–202
30. Politzer P, Murray JS (1991) Theoretical biochemistry and molecular biophysics: a comprehensive survey, vol 2. In: Beveridge DL, Lavery R (eds) Protein. Adenine , Schenectady, pp 165–191
31. Murray JS, Lane P, Brinck T, Politzer P, Sjoberg P (1991) Electrostatic potentials on the molecular surfaces of cyclic ureides. J Phys Chem 95:844–848
32. Muñoz-Caro C, Niño A, Sement ML, Leal JM, Ibeas S (2000) Modeling of protonation processes in acetohydroxamic acid. J Org Chem 65:405–410
33. Politzer P, Murray J, Concha MC (2002) The complementary roles of molecular surface electrostatic potentials and average local ionization energies with respect to electrophilic processes. Int J Quantum Chem 88:19–27